we make the substitution $\mathbf{p}=\mathbf{K}+\mathbf{q}$ where $\mathbf{K}=\frac{1}{2}(\mathbf{k}_0+\mathbf{k})$. Then

$$G(\mathbf{r},\mathbf{r}')=\exp[i\mathbf{K}\cdot(\mathbf{r}-\mathbf{r}')]\frac{1}{(2\pi)^3}\times\int\frac{\exp[i\mathbf{q}\cdot(\mathbf{r}-\mathbf{r}')]}{K^2+q^2+2\mathbf{K}\cdot\mathbf{q}-k^2-i\epsilon}(d\mathbf{q}). \quad (A.2)$$

At high energies, by assuming that

$$K^2-k^2=k^2(\cos^2\tfrac{1}{2}\theta-1)=-k^2\sin^2\tfrac{1}{2}\theta\approx-q^2 \quad (A.3)$$

and taking the z axis parallel to $\mathbf{K}$, we obtain

$$G(\mathbf{r},\mathbf{r}')\approx\exp[i\mathbf{K}\cdot(\mathbf{r}-\mathbf{r}')]\frac{1}{16\pi^3k}\times\int\frac{\exp[i\mathbf{q}\cdot(\mathbf{r}-\mathbf{r}')]}{q_z-i\epsilon}(d\mathbf{q}) \quad (A.4)$$

and when evaluated in cylindrical coordinates for positive $\epsilon\rightarrow 0$, this becomes

$$\begin{aligned} G(\mathbf{r},\mathbf{r}')&\approx\tfrac{1}{2}ik^{-1}\exp[i|\mathbf{K}|(z-z')]\delta(\boldsymbol{\varrho}-\boldsymbol{\varrho}'), & z>z',\\ G(\mathbf{r},\mathbf{r}')&\approx 0, & z<z'. \end{aligned} \quad (A.5)$$

PHYSICAL REVIEW VOLUME 95, NUMBER 2 JULY 15, 1954

Ionization Chamber Measurements at 10 600 Feet of the Absorption of the *N* Component in Carbon and Hydrocarbon*

ROBERT H. REDIKER†
Department of Physics and Laboratory for Nuclear Science, Massachusetts Institute of Technology, Cambridge, Massachusetts
(Received April 12, 1954)

A detector consisting of a lead-shielded ionization chamber with Geiger counters above and below the chamber is described. The charged N component of energy of several tens of Bev is detected.

The absorption of the charged N component in carbon is much smaller than that predicted from the absorption in air. This phenomenon may be explained by the fact that π mesons or other unstable particles which are produced in nuclear interactions can give rise to further nuclear interactions.

Approximate values for the interaction mean free path of N rays in carbon have been obtained. These values depend on the number of shielded counters below the ionization chamber which are struck. For zero counters discharged, the mean free path is 136 ± 12 g cm^{-2} and seems to decrease as the requirement on the number of shielded counters struck is increased. The interaction mean free paths in carbon are compared to previous results in lead.

The absorption of the N component in oil indicates a cross section of the hydrogen nucleus much smaller than that corresponding to the range of nuclear forces.

Events with large pulses from the ionization chamber or with multiple discharge of shielded counters below the chamber are more likely to be associated with the nucleonic component of extensive air showers.

I. INTRODUCTION

THE results reported here were obtained in a continuation of previous experiments[1–6] performed with a lead-shielded ionization chamber and an array of Geiger-Mueller counters above the lead shield. The time coincident pulses of the ionization chamber and of the Geiger counters recorded the arrival of penetrating ionizing particles which could produce ionization bursts below the lead shield. In a preceding paper[6] (referred to in what follows as I) we were able to separate the total burst rate recorded by the detector into two parts: one which arises from electromagnetic interactions of μ mesons, and another which arises from nuclear interactions of the so-called N component of cosmic rays.

The reader is referred to I for a discussion of the processes by which the bursts are produced. From the latitude effect observed with similar apparatus[5] and from correlation of the observed counting rate with the energy spectrum of the producing radiation, the mean energy of the detected radiation is determined to be about 10^{10} ev. This is in agreement with the energy transfer necessary to produce the smallest detected ionization burst (see I).

In the experiment described in I, we measured the absorption in air and in lead of the N component responsible for the detected bursts. We also obtained information about the collision mean free path for this radiation in lead.

In the present experiment, performed at 10 600 feet, we have extended the results of I to carbon and hydrocarbon absorbers. We have also investigated the absorption of the N component associated with extensive air showers.

* This work was supported in part by the joint program of the U. S. Office of Naval Research and the U. S. Atomic Energy Commission.

† Now at Lincoln Laboratory, Massachusetts Institute of Technology, Cambridge, Massachusetts.

[1] Bridge, Rossi, and Williams, Phys. Rev. **72**, 257 (1947).
[2] Bridge, Hazen, and Rossi, Phys. Rev. **73**, 179 (1948).
[3] Bridge, Hazen, Rossi, and Williams, Phys. Rev. **74**, 1083 (1948).
[4] H. Bridge and B. Rossi, Phys. Rev. **75**, 810 (1949).
[5] McMahon, Rossi, and Burdett, Phys. Rev. **80**, 157 (1950).
[6] H. Bridge and R. Rediker, Phys. Rev. **88**, 206 (1952).

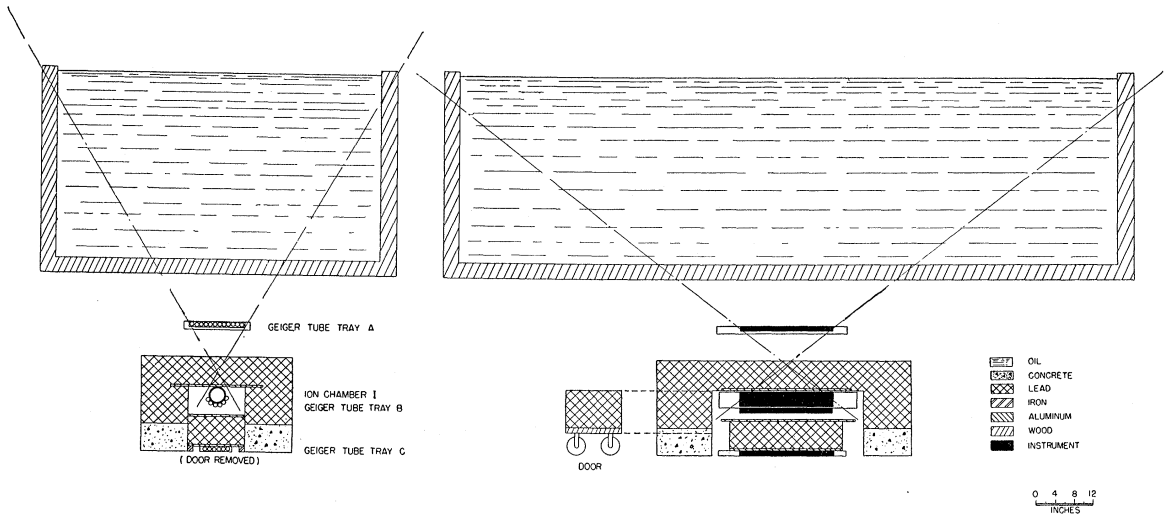

FIG. 1. Experimental arrangement showing full 85.5-g cm^{-2} oil absorber.

II. EXPERIMENTAL ARRANGEMENT

With one exception, the experimental arrangement shown in Fig. 1 was identical to the arrangement used in I at 10 600 feet. The one difference was that in this experiment 171 g cm^{-2} of lead rather than 142 g cm^{-2} of lead was placed between tray A and the ionization chamber. This lead served as the producing layer for most of the bursts observed in the ionization chamber. Not shown in Fig. 1 is the extension tray E, a counter tray of 0.15 square meters placed 3 meters from the detector and at the same height as the lower counter in tray B.

TABLE I. The coincidences whose rates were investigated as a function of absorber thickness.[a,b]

AI	Coincidence between pulse in Geiger Tray A and ionization burst in chamber.
AIB	Coincidence between pulses in Geiger Trays A and B and ionization burst in chamber.
A_1IB	Same as AIB except that only one Geiger tube in Tray A was struck.
$AIBC$	Coincidence between pulses in Geiger Trays A, B, and C and ionization burst in chamber.
A_1IBC	Same as $AIBC$ except that only one Geiger tube in Tray A was struck.
$AIBC_0$	Coincidence between pulses in Geiger Trays A and B and ionization burst in chamber, in anticoincidence with pulse from Tray C.
A_1IBC_0	Same as $AIBC_0$ except that only one Geiger tube in Tray A was struck.
$AIBC_1$	Same as $AIBC$ except that only one Geiger tube in Tray C was struck.
A_1IBC_1	Same as $AIBC$ except that only one Geiger tube in each of the Trays A and C was struck.
$AIBC_2$	Same as $AIBC$ except that at least two Geiger tubes in Tray C were struck.
A_1IBC_2	Same as $AIBC$ except that at least two Geiger tubes in Tray C were struck and only one Geiger tube in Tray A was struck.

[a] The symbol E after any of the coincidences listed above indicates a simultaneous pulse in the extension Geiger Tray E. Thus $AIBE$ is a coincidence between pulses in Geiger Trays A, B, and E and ionization burst in the chamber.

[b] The size of ionization-burst voltage pulses from the chamber are given in terms of the voltage pulse caused by a polonium α particle (5.30 Mev) near the wall of the chamber. The relative size is indicated by the subscript following I. I_m means the voltage due to the ionization burst was larger than m times the pulse due to the polonium α particle.

Directly above tray A one could stack different thicknesses of carbon or place a wooden tank which could be filled with different amounts of oil.

In what follows we shall concern ourselves with the various categories of events listed in Table I. In interpreting the results obtained for these events the following characteristics of the detector should be kept in mind. Requiring a coincidence between the ionization chamber I and a counter in tray B excluded low-energy interactions whose secondary particles failed to emerge from the wall of the ionization chamber. Requiring a coincidence between I and more than one C counter insured that the event causing the ionization burst in I was one in which penetrating particles were produced. In this manner, as we have shown in I, we are able to detect the N component alone. A coincidence with a counter in the extension tray, E, indicated that the detected event was associated with an air shower. It was shown in I and is evident from the results to be presented here that these events are produced by interactions of the penetrating particles in air showers.

III. RESULTS

(1) The Experimental Data

Coincidence rates have been obtained for the various categories of events listed in Table I for four thicknesses of the carbon absorber and four thicknesses of the oil absorber. These rates have been corrected for fluctuations in barometric pressure. The maximum barometric correction was of the order of six percent. The coincidence rates have also been corrected for accidental electronic coincidences and for overlap of pen marks on the recording tape from which most of the data were obtained (see I). Both these corrections are of the order of one percent and tend to cancel since they are of opposite sign.

In addition, the coincidence rates which arise from electromagnetic interactions of μ mesons (to be called

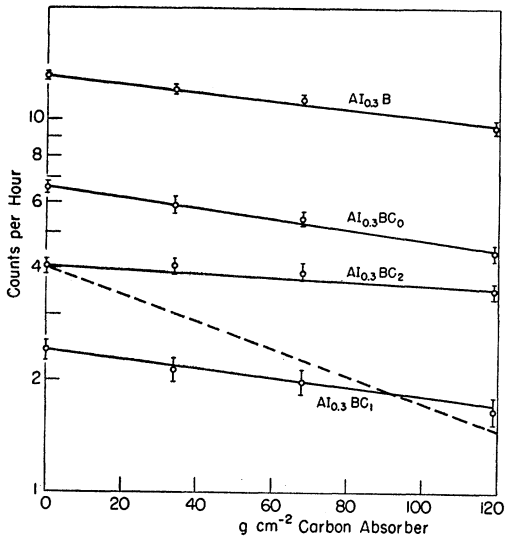

FIG. 2. The coincidence rate due to N bursts is plotted as a function of the carbon absorber thickness for the $AI_{0.3}B$, $AI_{0.3}BC_0$, $AI_{0.3}BC_1$, and $AI_{0.3}BC_2$ events. The dashed line shows the absorption $e^{-x/117}$ that would be expected from the model of the semitransparent nucleus and from the experimental value of the absorption thickness in air.

μ bursts) have been separated from the coincidence rates which are due to interactions of the N component (to be called N bursts). The method by which this separation was accomplished has been discussed in detail in paper I.

(2) Absorption of the N Component in Carbon

Figure 2 shows semilogarithmic plots of the coincidence rates due to N bursts as a function of absorber thickness for the $AI_{0.3}B$, $AI_{0.3}BC_0$, $AI_{0.3}BC_1$, and $AI_{0.3}BC_2$ events. (See Table I for an explanation of the symbols used to describe the different events.)

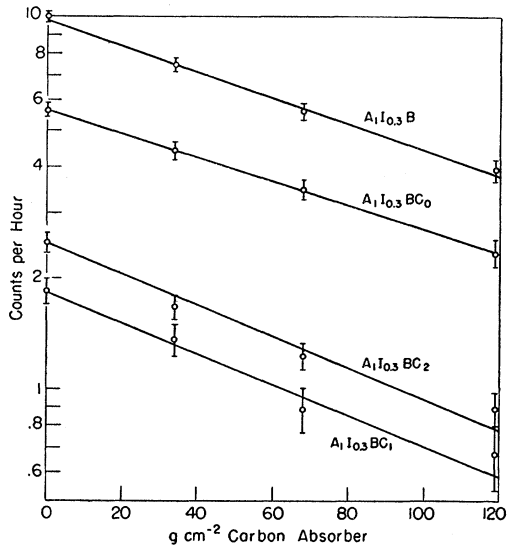

FIG. 3. The reduction of the $A_1I_{0.3}$ type of coincidence rates due to N bursts with addition of carbon absorber.

If one assumes that air and carbon absorbers differ only because of the small change in nuclear radius, one can calculate, using the model of the semitransparent nucleus, the expected absorption in carbon from the experimental absorption in air.[7] Taking the absorption thickness of the N component in air as 120 g cm^{-2} (this is consistent with the results in I and with those of other experimenters), one computes an expected exponential absorption in carbon with absorption thickness close to 117 g cm^{-2}. The dashed line in Fig. 2 shows this expected absorption. It is evident that the experimental absorption is much smaller than that predicted. A similar result was reported in I for lead.

The discrepancy between the absorption in carbon and in air is striking because of the similarity in size of the nuclei of carbon and air. The most likely explanation for this discrepancy is that π mesons (and/or any other unstable secondary particles) produced in high-energy nuclear interactions give rise to further nuclear interactions which produce the observed coincidences. While in air a large percentage of these π mesons decay before colliding with nuclei, in carbon almost all of them will interact before decaying. Thus the total number of interacting particles is greater under an air-plus-carbon absorber than under an equivalent thickness of air alone.[8]

(3) The Collision Mean Free Path of the N Component in Carbon

In this section we shall discuss the variation with absorber thickness of the rates of those coincidence events in which one and only one counter in tray A was struck (A_1 events). This requirement rules out many detected events in which the incident particle has interacted in the absorber. If all events associated with interactions in the absorber could be eliminated from the data, the measured absorption would yield directly the collision mean free path of the incident radiation. It seems likely that the above condition is not completely satisfied by the A_1 requirement (see I), and thus the measured mean free paths are somewhat longer than the actual collision mean free paths.

Figure 3 shows semilogarithmic plots of the coincidence rates due to N bursts as a function of carbon absorber thickness for the $A_1I_{0.3}B$, $A_1I_{0.3}BC_0$, $A_1I_{0.3}BC_1$, and $A_1I_{0.3}BC_2$ events. The mean free paths have been determined from a least-squares

[7] See B. Rossi, *High Energy Particles* (Prentice-Hall, Inc., New York, 1952) for a detailed discussion of this point.

[8] Another possible explanation for the difference in the absorption curves in air and condensed materials is the geometric coherence of particles produced in the condensed absorber. A nuclear interaction that takes place in the absorber may produce two or more secondary particles which then produce the observed coincidence only because of their striking the detecting equipment simultaneously. If the same interaction occurred in air, the secondary particles would in most cases be so widely separated at the detector that no such coincidence would be possible. An experiment investigating this effect was reported in I. The results show that this explanation is most unlikely.

treatment of the data under the assumption of an exponential decrease of the rates with absorber thickness. These mean free paths, shown in Table II, are larger than the collision mean free paths in carbon of 65–100 g cm^{-2} which have been reported for charged particles which produce penetrating showers.[9–11]

In order to reduce lifetime effects in the comparison of the results obtained in I with lead absorber and those obtained above with carbon absorber, wood spacers were inserted between the layers of lead absorber (see I). In this manner the effective density of the lead absorber was reduced to 5.16 g cm^{-3}. Table II compares the mean free paths in carbon, computed from the experimental absorption in lead according to the model of the semitransparent nucleus,[7] with the

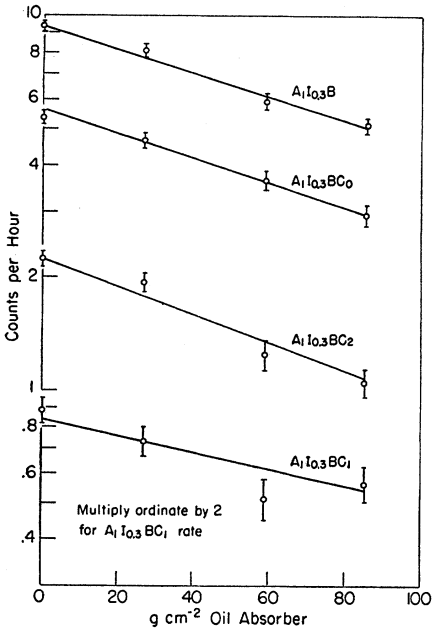

FIG. 4. The reduction of the $A_1I_{0.3}$ type of coincidence rates due to N bursts with addition of oil absorber.

experimental carbon results. Only the mean free paths for the $A_1I_{0.3}BC_0$ coincidence rates seem to be consistent with this nuclear model. This may indicate an experimental difficulty rather than a shortcoming of the nuclear model. Figure 8 of I and Fig. 3 show that in both lead and carbon, the absorption of the $A_1I_{0.3}BC_0$ coincidence rate can be fit very well by an exponential. On the other hand these two figures show that in lead and carbon, exponential absorption curves for the $A_1I_{0.3}BC_1$ and $A_1I_{0.3}BC_2$ rates are not fit well by the experimental points. It may be that the A_1 requirement for these events is not sufficient to eliminate the effects of secondary particles produced in the absorber.

[9] G. Cocconi, Phys. Rev. **76**, 984 (1949).
[10] Walker, Walker, and Greisen, Phys. Rev. **80**, 546 (1950).
[11] R. R. Brown, Phys. Rev. **87**, 999 (1952).

TABLE II. The mean free paths in g cm^{-2} of carbon or lead for the various $A_1I_{0.3}B$ type events under the assumption that the rates associated with N bursts vary exponentially with absorber thickness.

Absorber	$A_1I_{0.3}BC_0$	$A_1I_{0.3}BC_1$	$A_1I_{0.3}BC_2$
Carbon	136±12	122±22	111±11
Lead (from I)	225±14	292±41	286±23
Carbon calculated from results in lead	154_{-18}^{+20}	226±43	220±24

(4) Comparison of Results with Oil and Carbon Absorbers. The Interaction of the N Component with Hydrogen

Figure 4 shows semilogarithmic plots of the coincidence rates due to N bursts as a function of oil absorber thickness for the $A_1I_{0.3}B$, $A_1I_{0.3}BC_0$, $A_1I_{0.3}BC_1$, and $A_1I_{0.3}BC_2$ coincidences. Assuming an exponential decrease of the rates with absorber thickness, the mean free paths have been determined from a least-squares treatment of the data. Since these coincidences require that only one tube in tray A be discharged, these mean free paths given in Table III(*e*) are approximations to the interaction mean free paths in oil of the charged N rays incident from the atmosphere (see Sec. III. 3).

From the experimental data on the carbon absorption we have computed the collision mean free path in oil[12] under the following assumptions on the interaction cross section, σ_{Np}, between the particles of the N component and hydrogen nuclei: (a) $\sigma_{Np}=0$; (b) $\sigma_{Np}=25\times10^{-27}$ cm^2 (this corresponds to the cross section for p-p scattering at several hundred Mev); (c) $\sigma_{Np}=60\times10^{-27}$ cm^2 (this corresponds to a proton radius $r=\hbar/m_\pi c$, where m_π is the mass of the π meson); (d) σ_{Np} as determined for the different events from the absorption in carbon and the model of the semitransparent nucleus assuming $\sigma_{Np}=\sigma_{Nn}$,[13] i.e., assuming the interaction cross section of the N rays with neutrons and protons to be equal.

TABLE III. The mean free paths in g cm^{-2} of oil for the various $A_1I_{0.3}B$ type coincidences under the assumption that the rates associated with N bursts vary exponentially with absorber thickness. Mean free paths calculated from the results in carbon and with various assumed hydrogen interaction cross sections are compared with the experimental result.

	$A_1I_{0.3}BC_0$	$A_1I_{0.3}BC_1$	$A_1I_{0.3}BC_2$
(a) Calculated with $\sigma_{Np}=0$	156±14	140±25	128±13
(b) Calculated with $\sigma_{Np}=25\times10^{-27}$ cm^2	121±8	110±16	102±8
(c) Calculated with $\sigma_{Np}=60\times10^{-27}$ cm^2	90±5	85±9	80±5
(d) Calculated with σ_{Np} as determined from experimental absorption in carbon	129±13	115±23	104±12
(e) Experimental	146±16	167±38	108±12

[12] The chemical analysis of the diesel oil used as absorber was by weight: hydrogen 13.1 percent, carbon 84.0 percent, oxygen 2.6 percent, and sulfur 0.3 percent.
[13] These cross sections are (17.2±2.1, 20.2±5.6, 23.5±3.9) $\times10^{-27}$ cm^2 for the $A_1I_{0.3}BC_0$, $A_1I_{0.3}BC_1$, and $A_1I_{0.3}BC_2$ events, respectively.

The results are compared in Table III with the experimental findings. One sees that while any of the assumptions (a), (b), or (d) is consistent with the experimental data, assumption (c) is ruled out. We thus conclude that the cross section for interaction of N particles with protons is not much larger than 25×10^{-27} cm^2 and could be zero.

Two uncertainties must be kept in mind in interpreting this result. First, if the energy and angular distribution of secondaries produced when the N component interacts with carbon nuclei are very different from those resulting when it interacts with hydrogen nuclei, then the efficiency of detecting an interaction in the absorber might be quite different for the two kinds of interactions. If in the interactions with hydrogen nuclei the secondaries are emitted in a very narrow cone in the laboratory system, it is conceivable that all the secondary particles could pass through a single counter in tray A and the interaction would be missed. In this case the experimental cross section would be too small. Similarly, the requirement that only one counter in tray A be discharged would not eliminate elastic scattering,[14] including charge exchange, of neutrons by the hydrogen nuclei in the absorber. Experimentally there is very little information either on the angular distribution of the secondary particles emitted in nucleon-nucleon collisions or on the possibility of elastic scattering. While the present experiment can give no indication as to elastic scattering, if the angular distribution is to explain the small observed cross section for the interaction of N particles with protons, the secondaries must be concentrated in a cone of half-angle smaller than 1.1 degrees. (This is the half-angle subtended by a counter in tray A at the middle of the oil absorber.)

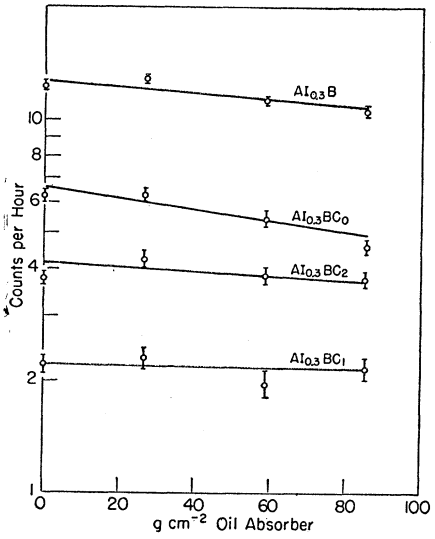

FIG. 5. The coincidence rate due to N bursts is plotted as a function of oil absorber thickness for the $AI_{0.3}$ type of events.

[14] By elastic scattering we mean scattering in which no new particles are produced.

Secondly, one should realize that the interaction cross sections determined for carbon above and for lead in I are considerably smaller than the corresponding cross sections determined with penetrating shower detectors (see Sec. III. 3 and paper I). While part of this discrepancy may be caused by the general inadequacy of the A_1 requirement in ruling out all events in which the incident particle interacts in the absorber, it is difficult to explain the entire discrepancy on this basis.

Figure 5 shows semilogarithmic plots of the coincidence rates due to N bursts as a function of oil absorber thickness for the $AI_{0.3}B$, $AI_{0.3}BC_0$, $AI_{0.3}BC_1$, and $AI_{0.3}BC_2$ coincidence events. A comparison of Figs. 5 and 4 with the corresponding Figs. 2 and 3 for absorption in carbon indicates that regardless of whether or not we require that only one counter be discharged in tray A, the absorption in oil is consistent with the absorption in carbon under the assumption that the N component does not interact with the hydrogen nucleus.

(5) Events Associated with Air Showers

Figure 6 shows logarithmic plots of the coincidence rates as a function of both carbon and oil absorber thickness for the $AI_{0.3}BE$, $AI_{0.3}BC_0E$, $AI_{0.3}BC_1E$, and $AI_{0.3}BC_2E$ coincidences. For these air-shower associated events, no separation has been made into μ bursts and N bursts. A comparison of Figs. 2 and 5 with Fig. 6

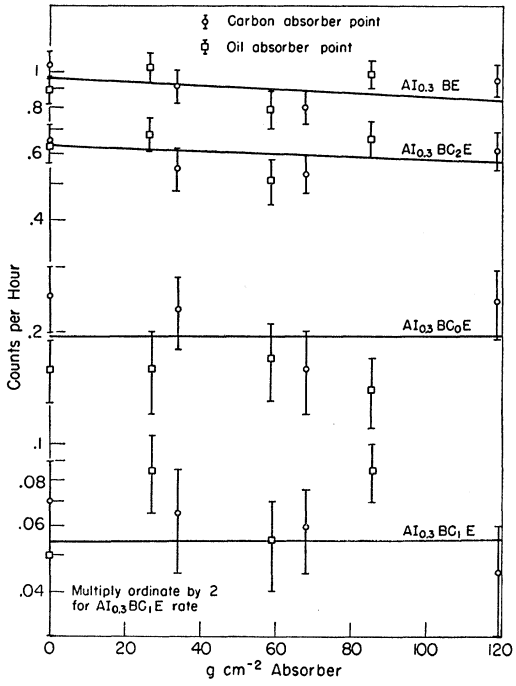

FIG. 6. The coincidence rate is plotted as a function of the oil absorber thickness and the carbon absorber thickness for the events associated with air showers, $AI_{0.3}BE$, $AI_{0.3}BC_0E$, $AI_{0.3}BC_1E$, and $AI_{0.3}BC_2E$. For these events, no separation has been made into N bursts and μ bursts.

shows that the variation of the rates with absorber thickness is independent within statistics of the requirement that the events be associated with an air shower. This result is in agreement with the conclusion reached in I that these events associated with the discharge of counters in the extension tray are due to the N rays in air showers.[15–17] While the electrons discharge the extension tray, the N rays through their nuclear interactions give rise to the AIB coincidences as in the case of unassociated events.

Two or more counters in the shielded tray C were struck in 65 percent of the $AI_{0.3}B$ events associated with air showers, but were struck in only 30 percent of the $AI_{0.3}B$ events not associated with air showers. This result is in agreement with other observations showing that large penetrating showers are more frequently associated with air showers than are small penetrating showers.[17]

The rate of events associated with air showers in which only one tube in tray A is struck ($A_1I_{0.3}BE$ events) is negligible, as would be expected.

Since the events associated with air showers are believed to be due to the N component, they have not been subtracted from the coincidence rates. An analysis of the data in terms of unassociated events would not alter any of the conclusions we have obtained above.

[15] Cocconi, Tongiorgi, and Greisen, Phys. Rev. **75**, 1063 (1949).
[16] G. Cocconi and V. C. Tongiorgi, Phys. Rev. **79**, 730 (1950).
[17] Greisen, Walker, and Walker, Phys. Rev. **80**, 535 (1950).

(6) The Pulse-Height Distribution

Data were also obtained for the events listed in Table I for different minimum voltage pulses from the ionization chamber. In addition to the coincidences with the $I_{0.3}$ pulses, results were obtained for coincidences with $I_{0.6}$, $I_{0.9}$, $I_{1.2}$ pulses (see Table I for definition of these terms). In agreement with I these results indicate that within the experimental errors the shape of the pulse-height distributions for a given coincidence event is independent of the absorber thickness. Thus the pulse-height distributions given in I apply here.

The pulse-height distributions for events associated with air showers are much flatter than those for events not associated with air showers. Thus, while only (6.7 ± 0.6) percent of the $AI_{0.3}B$ coincidences are associated with air showers, (14 ± 2) percent of the $AI_{1.2}B$ coincidences are associated with air showers.[18]

The experiment discussed in this paper was performed at the Inter-University High Altitude Laboratory at Echo Lake, Colorado. The author wishes to thank Professor Bruno Rossi for his continual and generous help and encouragement. Much of the apparatus was designed by Dr. H. S. Bridge, whose continued interest in this work is greatly appreciated. The author was fortunate in having the assistance of Mr. Daniel T. Anderson in performing the experiment.

[18] These results are for 0 g cm^{-2} oil absorber.

PHYSICAL REVIEW VOLUME 95, NUMBER 2 JULY 15, 1954

Cosmic Radiation at Very High Altitudes Near the Geomagnetic Equator*

MARTIN A. POMERANTZ†
Bartol Research Foundation of the Franklin Institute, Swarthmore, Pennsylvania

(Received March 16, 1954)

During an extensive series of balloon-flights near the geomagnetic equator in India, intensity-depth curves have been obtained with the standard quadruple coincidence counter trains, containing various thicknesses of interposed absorber (4.0 cm, 7.5 cm, and 17.7 cm of Pb), previously utilized at high latitudes. A rather pronounced difference occurs between the two stations at Aligarh, Uttar Pradesh ($\lambda=18°$ N) and Bangalore, Mysore ($\lambda=3°$ N). The primary flux values, extrapolated to the "top of the atmosphere" from data obtained with instruments containing 7.5 cm of Pb, are 0.032 ± 0.001 and 0.024 ± 0.001 cm^{-2} sec^{-1} sterad^{-1}, respectively.

A maximum appears in all of the curves, and the general features, as well as the absorption characteristics of the cosmic rays in the upper atmosphere, are in accord with expectation. The effective absorption length in lead, approximately 290 g cm^{-2}, remains unchanged when the geomagnetic cut-off energy of the primary protons is increased from 1.4 Bev to 14.2 Bev. The intensity of mesons having energies exceeding 260 Mev is determined from the data by invoking Messel's theory of the nucleon cascade, and this yields results which are in excellent agreement with the available experimental facts.

The primary magnetic-rigidity spectrum averaged over the range 2.1 Bv to 15.4 Bv is $N(>pc/Ze)=0.68(1+pc/Ze)^{-1.2}$, based upon the present measurements at 52° N and 3° N. However, the data recorded within the equatorial region require a higher value of the corresponding exponent in the differential distribution if the usual assumptions are valid. This effect may be attributable to an irregularity in the primary spectrum, contributions from trapped orbits and albedo, or local magnetic anomalies.

The ratio of intensities in the horizontal and vertical directions at high altitudes is practically equal at 52° N and 3° N, although it would have been expected to increase near the equator in view of the decrease previously observed north of 52°.

I. INTRODUCTION

INVESTIGATIONS of the variation with latitude of the intensity and properties of various components of the cosmic radiation have yielded a considerable amount of information regarding the primary particles. In particular, the only direct method available for the

* Assisted by the U. S. Office of Naval Research and by the U. S. Atomic Energy Commission. Field expedition sponsored by National Geographic Society.

† Fulbright Professor, Muslim University, Aligarh, U. P., India, 1952–53.